Journal of Marine Research, 57, 739–761, 1999

Strange encounters of eddies with walls

by Doron Nof[1]

ABSTRACT

The impingement of a westward drifting lens-like anticyclonic ring on a meridional boundary is examined analytically and numerically using an (inviscid) layer-and-a-half model. A nonlinear analytical solution is constructed with the aid of a slowly varying perturbation expansion and numerical simulations are performed with the Bleck and Boudra model.

It is found that, in contrast to conventional wisdom which implies that an anticyclonic ring encountering a wall moves poleward due to the image effect, the ring stays roughly in a fixed latitude. As it slowly moves into the wall due to β, it gradually leaks fluid toward the equator until it loses all of its mass. As expected, different eddies lose their mass in different rates. The (nondimensional) central thickness of an intense zero potential vorticity ring decays as $1/[1 + \beta(2g'H_i)^{1/2}\ t/18f\,]^2$ where H_i is the initial central thickness, t is time, g' the "reduced gravity," f the Coriolis parameter, and β is the familiar variation of the Coriolis parameter with latitude. Due to the gradually decreasing depth, the ring's westward drift into the wall also gradually slows down; i.e., the ring advances toward the wall and loses mass like a gradually peeling onion. The "peeling" rate is $2\beta R_d^2/9$ [where R_d is the instantaneous Rossby radius based on the instantaneous maximum thickness] implying that the eddy migrates toward the wall at a rate that is one-third of the free open ocean rate.

Numerical simulations are in excellent agreement with the above solution. As expected, they show that frictional forces decrease the intensity of the leakage and, hence, slow down the draining process. Unfortunately, no analytical solution can be found for weak or moderately strong rings because, for such lenses, there is no known analytical solution even for the nonmigrating state (i.e., rings on an f-plane). Numerical simulations show, however, that such weak or moderately strong rings display (qualitatively) similar characteristics to those of intense zero potential vorticity rings.

It is argued that rings such as warm-core Gulf Stream rings, Loop Current rings, Agulhas rings, as well as other eddies (e.g., Meddies) may all experience similar encounters. As the walls that they encounter are subsurface (e.g., the continental rise, the Walvis Ridge and the mid-Atlantic Ridge), the leakages are not expected to be easily detected.

1. Introduction

The question of what happens when an anticyclonic ring encounters a vertical western boundary has frustrated some oceanographers for decades. Despite quite extensive efforts, there is no agreement today even on such basic issues as whether the rings should migrate poleward or equatorward once they encounter the wall (see, e.g., Shi and Nof (1993, 1994) and the references therein). Our present interest in the problem is enhanced by two issues.

1. Department of Oceanography and Geophysical Fluid Dynamics Institute, The Florida State University, Tallahassee, Florida, 32306-4320, U.S.A. ***email: nof@ocean.fsu.edu***

First, because of the climatically relevant eddy-induced meridional transfer of heat, mass, and salt, the problem is of more practical importance today than it was when it was first considered (in the early eighties). Second, there have been many new observations since the eddy-wall problem was first considered and these may help understand the problem. For instance, there have been recent observations of Meddies interacting with seamounts (Richardson and Tychensky, 1998) suggesting that Meddies are sometimes destroyed after they encounter meridional boundaries.

We refer to the eddy-wall encounters as "strange encounters" because, as we shall see, they exhibit counter-intuitive patterns. In particular, instead of migrating along the wall (which is the behavior expected from simple principles), the eddy stays in an almost fixed latitude. It gradually loses its mass via a leakage until it completely loses its identity as a coherent feature. We shall focus our attention on a particular kind of eddy which is bounded by an interface that strikes the surface enclosing a finite amount of anomalous fluid. This eddy, whose shape is like a lens, is highly nonlinear (due to the large thickness variations) but is relatively easy to examine because all motions are confined to the eddy itself. Namely, since there is no fluid of the eddy density around it, no radiation is possible and the fluid surrounding the eddy is always at rest. (Hereafter, we shall use the terms "ring," "vortex" or "eddy" interchangeably; all will imply reference to the particular kind of eddy mentioned above.) In addition to limiting ourselves to an eddy-lens, we shall focus on (intense) eddies with zero potential vorticity (i.e., steep eddies with a linear velocity profile whose gradient is $-f/2$) because such eddies are robust and can be handled analytically. Furthermore, these eddies seem to adequately represent actual rings such as warm-core Gulf Stream rings (see, e.g., Olson, 1991).

We shall also focus on a vertical wall even though it is not at all obvious that a vertical wall is the appropriate representation of the oceanic boundary. This is because eddies frequently encounter a weakly sloping bottom rather than a vertical wall. Nevertheless, the actual bottom slope is often much steeper than the slope of the lens' interfacial boundary, making the vertical boundary approximation plausible for some cases.

a. Background. It has been known for some time now that the eddy-wall problem involves three subprocesses. The first, and most familiar aspect, is the so-called image effect which arises from the fact that next to the boundary the streamlines must adjust to the boundary shape and become meridional. Satisfaction of the latter condition is achieved when the vortex "sees" its image vortex behind the wall. By mutual advection, such an image implies a poleward migration of anticyclonic rings (see, e.g., Minato, 1982, 1983; Yasuda *et al.,* 1986; Masuda *et al.,* 1987; Masuda, 1988; Umatani and Yamagata, 1987). We shall see that, because the influence of β on the lens is small (at any given moment), the distance that the lens eddy is forced into the wall is small compared to the Rossby radius. Consequently, the motions introduced by the mirror vortex are small and negligible. The second subprocess is the tendency of the rings to be pulled equatorward by the β-induced southward force which is no longer balanced by the northward Coriolis force once the wall

is encountered and the ring's westward drift is reduced. The third subprocess is the tendency of the ring to be pushed poleward due to the rocket effect associated with the leakage that is established along the wall (see, e.g., Nof, 1988a,b; Shi and Nof, 1993, 1994). How the ring finally behaves depends on the competition between these three processes. Although the existence of the above three subprocesses has been known for some time, there has not been any case for which all three were computed analytically in detail. Shi and Nof 's (1994) analytical solution involves a quasi-geostrophic eddy that does not leak and Nof (1988a,b) involves quasi-geostrophic eddies that leak but are not subject to β. Here, we present the first nonlinear solution that involves all three processes together. (Note that since, by definition, a lens is always nonlinear, the quasi-geostrophic limit of our solution cannot be taken.)

As mentioned, we shall see that in our intense lens-like eddies case, the image effect is relatively small and negligible (because of the small shape distortions). By contrast, the two other effects are large. Surprisingly, however, it turns out that they almost cancel each other. Consequently, the lens becomes quasi-stationary and is gradually losing its mass (via the leakage). As mentioned, although the presence of each of the three subprocesses has been known for some time, it has not been clear at all how the three processes combine together nor has it been clear how to compute them. Consequently, it has not been clear where the rings migrate to after encountering the wall nor has it been clear what controls the leakage. Here, we derive the first complete time-dependent analytical solution for nonlinear lens-like eddies. It provides the answers to the above questions; i.e., it tells us whether or not the ring is migrating and it tells us the rate at which the ring loses its mass.

b. Present approach. Consider the situation shown in Figure 1. Our approach is to look at the eddy-wall impingement process as a slowly varying problem. This is based on the idea that the process involves two time scales, a fast time scale and a slow time scale. The fast time scale [$O(f^{-1})$] is associated with the time required for a particle to complete a single revolution within the eddy whereas the slow time scale [$O(\beta R_{di})^{-1}$, where R_{di} is the initial Rossby radius] is the time associated with the eddy response to its impingement on the wall (which is roughly equal to its diameter divided by its westward migration rate). In this scenario the eddy is intense [i.e., its orbital speed corresponds to a Rossby number of $O(1)$] whereas the interaction with the wall is weak in the sense that it is associated with a slow forcing of the eddy into the wall. [Note, however, that this weak effect accumulates over a long time to become an $O(1)$ effect.] Since the only simple analytical solution for a lens-like eddy on an *f*-plane is the one for a zero potential vorticity eddy,[2] we shall limit ourselves to small potential vorticity eddies. With the above scales the eddy's draining time (i.e., the time that it would take the eddy to completely lose its identity as a coherent feature) is $O(\beta R_{di})^{-1}$.

2. Csanady (1979) derived an analytical solution for a finite potential vorticity lens, but the solution is not simple enough to be considered as a part of an involved perturbation expansion such as ours. Furthermore, it is inaccurate near the eddy's rim (Flierl, 1979).

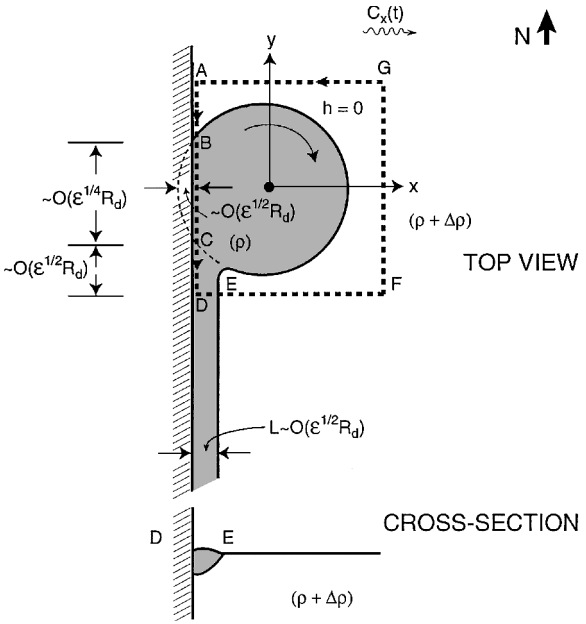

Figure 1. Schematic diagram of the model under study. The lens-like eddy drifts freely in the open ocean until it encounters the meridional wall. Subsequently, it leaks fluid along the wall and the westward migration is gradually reduced as the vortex progresses farther and farther into the wall. The "wiggly" arrow indicates the zonal migration of the vortex [$C_x(t)$]. The small parameter is defined by $\varepsilon \equiv \beta R_{di}/f$ (where R_{di} is the initial Rossby radius, i.e. the Rossby radius in the open ocean). Both the penetration distance into the wall and the thickness of the leaking jet are of $O(\varepsilon^{1/2}R_d)$; the geometry then implies that the length of the eddy's contact region with the wall (BC) is $O(\varepsilon^{1/4}R_d)$. The thick dashed line indicates the integration path that will be used. The thin dashed line indicates the eddy edge in the absence of the wall.

We shall consider the inviscid shallow water equations in a coordinates system traveling zonally with the eddy center at a gradually decreasing speed toward the wall (Section 2). We shall then consider the integrated balance of forces in the meridional direction and neglect all terms of order higher than ε (where $\varepsilon \equiv \beta R_{di}/f$). After some fairly tedious algebra and some not-so-obvious scaling, we find a very simple analytical solution for the eddy's reduction in size (Section 3). It shows that the encounter corresponds to a balance between the equatorward β-induced force, the poleward momentum-flux associated with the leak, and the poleward Coriolis force associated with the forever decreasing migration of the eddy's center toward the wall. In our calculations, the image effect is a higher-order process (which is not included) because it is associated with small perturbations to the eddy's circular shape (which are neglected).

Using a numerical "reduced gravity" model (of the Bleck and Boudra type) we shall then show (Section 4) that, as the analytical solution predicts, the eddy's radius shrinks. For completeness, we also run a numerical experiment with a weak eddy, i.e., an eddy that does

not possess two different time scales. We show that even this eddy corresponds roughly to the same balance of forces that the zero potential vorticity is subject to. Possible applications of the theory to various rings in the ocean are discussed and the results are summarized in Section 5.

2. Formulation

This section describes the physics of the problem and the mathematical approach. For clarity, the solution (which involves a perturbation's expansion) is presented in two stages. First, using the slowly varying process approach, we show that, in the momentum equations, all derivatives with respect to time can be ignored. (In the continuity equations, however, the derivatives with respect to time cannot be neglected *a priori.*) Using this information we then introduce a streamfunction and show that, to zeroth order, the *f*-plane eddy structure can be used to compute the forces. Because of the nature of our presentation, the usual procedure of formally nondimensionalizing all the terms at once and then performing an expansion is confusing and difficult to follow. It is much easier to retain the terms in dimensional form and examine their relative importance during each stage of the analysis. This is the manner in which the problem is presented below.

The reader is warned in advance that, even with this simpler presentation, it may be difficult and painful to follow the scaling and mathematical analysis in detail. To alleviate some of this pain, it is useful to *a priori* introduce the governing equations that we are after. We are after two conservation relationships. The first is the (straightforward) integrated conservation of eddy mass,

$$\frac{dV}{dt} = -q$$

where $V(t)$ is the eddy volume (slowly varying in time) and $q(t)$ is the (again slowly varying) draining mass flux via the leak. The second relationship that we seek is the not-so-simple conservation of meridional momentum-flux (or flow force),

$$\beta \iint \psi ds = C \iint fh ds + \text{rocket force due to leak}$$

where ψ is a streamfunction (in a coordinate system moving with the eddy center) and s is the vortex area. The term on the left is the southward (slowly decreasing) force due to β; it is balanced by the (gradually decreasing) northward Coriolis force (due to the westward migration of the lens) and the (slowly decreasing) northward rocket force due to the (equatorward) leak. Without a wall, there is no leak and the above relationship reduces to the familiar open ocean balance between the (steady) β force and the (steady) Coriolis force (see e.g., Nof, 1981). With the above presentation of the main governing equations, the reader who is primarily interested in the results can now go directly to the solution (3.3–3.7).

We shall now begin the detailed derivation of the governing equations. Consider a lens-like eddy drifting freely in the (infinitely deep) open ocean (Nof, 1981; Killworth, 1983) and reaching a meridional wall (Fig. 1) at $t = 0$. Once the inviscid vortex senses the

wall, its westward drift gradually slows down and it begins leaking fluid along the wall. First, as already mentioned, we note that the problem involves a "fast" time scale [$O(f)^{-1}$, i.e., days] and a "slow" time scale [$O(\beta R_{di})^{-1}$, i.e., weeks]. The "fast" time scale is associated with the (geostrophic) adjustment time scale and with the relatively short time that it takes a particle to complete a single revolution within the zero potential vorticity eddy. By contrast, the "slow" time scale [$O(\beta R_{di})^{-1}$ is associated with the slow westward drift toward the wall [$O(\beta R_{di}^2)$] which implies a slow eddy draining time [$\sim O(\beta R_{di})^{-1}$]. The small parameter $\varepsilon \equiv \beta R_{di}/f$ is the ratio between these short and long time scales. In what follows we shall consider the conservation of mass and momentum for the eddy-wall problem and examine the associated scales.

a. Conservation of mass. Assuming (and later verifying with our numerical experiments) that the flow is geostrophic downstream along the wall we find,

$$-\frac{d}{dt}\iint_S = \frac{g' h_c^2}{2 f_0}, \tag{2.1}$$

where h is the upper layer thickness, h_c is the thickness of the leakage along the wall at point C (see Fig. 1), S is the area of the entire vortex, and the remaining notation is conventional. Note that, for convenience, variables are defined both in the text and in the Appendix. The left-hand side of (2.1) is the volume rate of change whereas the right-hand side is the geostrophic transport of the leak. Since the volume change in time is long [i.e., $t \sim O(f^{1}/\varepsilon)$] we immediately see that h_c is $\sim O(\varepsilon^{1/2} H_i)$, where H_i is the initial central thickness.

b. Momentum flux. To examine the momentum-flux balance, we write the nonlinear momentum equations and the continuity equation in a coordinates system moving with the eddy center toward the wall,

$$h\frac{\partial u}{\partial t} + h\frac{\partial C_x}{\partial t} + hu\frac{\partial u}{\partial x} + hv\frac{\partial u}{\partial y} - (f_0 + \beta y) vh + \frac{g'}{2}\frac{\partial}{\partial x}(h^2) = 0 \tag{2.2a}$$

$$h\frac{\partial v}{\partial t} + hu\frac{\partial v}{\partial x} + hv\frac{\partial v}{\partial y} + (f_0 + \beta y)(u + C_x)h + \frac{g'}{2}\frac{\partial}{\partial y}(h^2) = 0 \tag{2.2b}$$

$$+\frac{\partial}{\partial x}(hu) + \frac{\partial}{\partial y}(hv) = 0, \tag{2.3}$$

where the momentum equations were multiplied by the eddy thickness, h, and, as before, the conventional notation is given in both the text and in the Appendix. Namely, u and v are the horizontal velocity components, C_x is the time-dependent migration rate in the x direction, g' is the "reduced gravity," and t is time. Note that (2.2–2.3) were obtained by applying the familiar transformation $x = \hat{x} - \int_0^{\hat{t}} C_x(t)\, d\hat{t}$); $y = \hat{y}$ $t = \hat{t}$ [where the variables with hats (ˆ) are associated with the fixed coordinate system and the absence of a hat denotes the variables in the moving system] to the usual time-dependent equations. In the

moving coordinate system the wall appears to be moving toward the eddy so that the wall boundary condition is

$$u = -C_x \text{ at } x = x_{\text{wall}} - \int_0^t (C_x\, dt).$$

Note also that we have ignored any migration along the wall; we shall see later that, although there is such a migration, it is $\sim[O(\varepsilon^{5/4}(g'H_i)^{1/2})]$ so that it is smaller than the speeds that we shall solve for $\sim[O(\varepsilon(g'H_i)^{1/2})]$. In what follows we shall keep terms up to a (relative) order of ε and show that, upon surface integration, the $O(1)$ terms drop out. Before getting into the details of this particular manipulation, the reader is warned again that, although an attempt has been made to make the presentation as simple as possible, this analysis may not be easy to follow.

We begin our detailed analysis by noting that, since $C_x \sim O[\varepsilon(g'H_i)^{1/2}]$ and the long variation in time due to β (which forces the eddy into the wall) is of $\sim O(f^1/\varepsilon)$, the term $h\,\partial C_x/\partial t$ is of $O[\varepsilon^2(g'H_i)^{1/2}H_i f]$ and, therefore, will be neglected. It will become clear later that, within the eddy, the fractions of u and v that vary on the slow time scale are, at the most, of $\sim O[\varepsilon^{1/2}(g'H_i)^{1/2}]$ so that, for the eddy, we can write

$$u(x, y, \varepsilon t) = \overline{u}(x, y) + \varepsilon^{1/2}u'(x, y, \varepsilon t) + \cdots \text{and } v(x, y, \varepsilon t) = \overline{v}(x, y) + \varepsilon^{1/2}v'(x, y, \varepsilon t) + \cdots$$

(where $\overline{u}$ and $\overline{v}$ are the speeds in the absence of the wall and u' and v' are the perturbations due to the encounter with the wall). This implies that, within the eddy, the terms $h\,\partial u/\partial t$ and $h\,\partial v/\partial t$ are, at the most, $O[\varepsilon^{3/2}(g'H_i)^{1/2}H_i f]$ so that they also are smaller than the terms that we shall keep $\{O[\varepsilon(g'H_i)^{1/2}H_i]f\}$ and, therefore, can be neglected.

Within the leak the velocity is of $O[(g'H_i)^{1/2}]$ and not of $O[\varepsilon^{1/2}(g'H_i)^{1/2}]$ because conservation of Bernoulli along the front ($h = 0$) implies that the speed along the eastern edge of the leak must be approximately equal to the orbital speed along the eddy's periphery. However, the thickness is now of $O(\varepsilon^{1/2}H_i)$ so that the term $h\,\partial v/\partial t$ is $O[\varepsilon^{3/2}H_i(g'H_i)^{1/2}f]$, and therefore will also be neglected within the leak.

Next we note that, since the entire eddy's thickness H varies in time, the term $\partial h/\partial t$ in the continuity equation is $\sim O(\varepsilon H_i f)$ within the eddy. On the basis of the above scaling we shall retain terms up to $O(\varepsilon)$ in both the momentum equations and the continuity equation. Namely, we neglect all derivatives with respect to time in the momentum equations but keep the time-dependent term in the continuity equation.

With this important simplification, (2.2b) is now integrated over the area bounded by the thick dashed line in Figure 1 noting that outside the eddy $h \equiv 0$. Using the continuity equation (2.3) (with the term $\partial h/\partial t$ intact) one finds,

$$\iint_S \left[\frac{\partial}{\partial x}(huv) + \frac{\partial}{\partial y}(hv^2)\right] dxdy + \iint_S v\,\frac{\partial h}{\partial t}\,dxdy + \iint_S (f_0 + \beta y)(u + C_x)\,h\,dxdy + \frac{g'}{2}\iint_S \frac{\partial}{\partial y}(h^2)\,dxdy = 0. \tag{2.4}$$

We now see that the second term can be neglected because $\partial h/\partial t$ is of (relative) order ε and the only asymmetrical part of v that can contribute to the integral over the eddy is of $O(\varepsilon)^{1/2}$, implying that the term is of $O(\varepsilon^{3/2})$. Note that, since the wall is moving toward the eddy, the integration area S is a (weak) function of time. This movement of the wall has no direct bearing on the calculation because all of the time-dependent terms are ignored.

Next we define the streamfunction ψ to be $\partial\psi/\partial y = -uh$; $\partial\psi/\partial x = vh$ and rewrite (2.4) as

$$\iint_S \left[\frac{\partial}{\partial x}(huv) + \frac{\partial}{\partial y}(hv^2)\right] dxdy - \iint_S (f_0 + \beta y)\frac{\partial \psi}{\partial y}\, dxdy + \iint_S (f_0 + \beta y)\, C_x\, h\, dxdy + \frac{g'}{2}\iint_S \frac{\partial}{\partial y}(h^2)\, dxdy = 0. \tag{2.5}$$

Note that, due to the nonzero $\partial h/\partial t$ term in the continuity equation, the function ψ is not exactly a constant along a streamline.

Eq. (2.5) can be rearranged and written as

$$\iint_S \left[\frac{\partial}{\partial x}(huv) + \frac{\partial}{\partial y}(hv^2)\right] dxdy - \iint_S f_0 \frac{\partial \psi}{\partial y}\, dxdy - \iint_S \left[\frac{\partial}{\partial y}(\beta y\psi) - \beta\psi\right] dxdy + C_x \iint_S (f_0 + \beta y)\, h\, dxdy + \frac{g'}{2}\iint_S \frac{\partial}{\partial y}(h^2)\, dxdy = 0, \tag{2.6}$$

and application of Stokes' theorem to (2.6) gives

$$\oint_\phi huvdy - \oint_\phi (hv^2 + g'h^2/2 - f\psi)\, dx + C_x \iint_S fhdxdy + \beta \iint_S \psi\, dxdy = 0 \tag{2.7}$$

where ϕ is the boundary of S and the arrowed circles indicate counterclockwise integration.

We now note that if there were no leak then ψ would be a constant along a streamline and we could have chosen it to be zero along the boundary which would then imply that $\oint f\psi dx = 0$. In reality there is a weak leak so that ψ is not exactly a constant along ϕ and the integral $\oint f\psi dx$ is not exactly zero. However, the largest gradient of ψ is within the leak where $\psi \sim O(\varepsilon g' H^2/f)$. Since the leak is narrow [$\sim O(\varepsilon^{1/2} R_d)$], the relative contribution of the term $\oint f\psi dx$ is of $O(\varepsilon^{3/2} g' H^2 R_d)$ and, therefore, can be neglected. Since within the leak $h \sim O(\varepsilon^{1/2} H)$, the integral $\int g' h^2/2\, dx$ across the leak is $\sim O(\varepsilon^{3/2}\, g' H^2 R_d)$ and, consequently, can also be neglected. We further note that at least one of the three variables h, u, and v vanishes on every portion of the boundary ϕ, so that (2.7) can be rearranged and written as,

$$-\int_D^E hv^2\, dx + C_x \iint_S (f_0 + \beta y)\, h\, dx\, dy + \beta \iint_S \psi\, dxdy = 0. \tag{2.8}$$

Eq. (2.8) represents a balance between three forces (Fig. 2). The first is a northward force associated with the leak. It is analogous to the force produced by a rocket or a sprinkler.

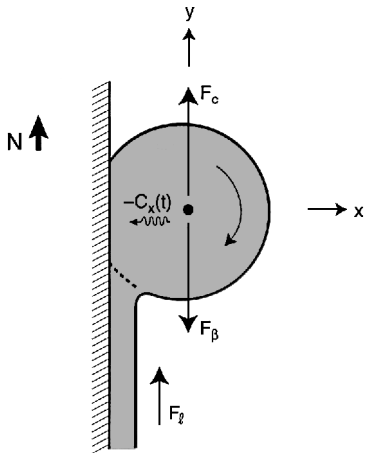

Figure 2. The balance of forces acting on an intense lens-like vortex encountering a wall. Both the integrated Coriolis force Fc (resulting from the eddy's forever slowing migration toward the wall) and the integrated "rocket force" F_l (resulting from the leak) are pointing poleward. They balance the equatorward β-induced force (resulting from the fact that each particle senses a different Coriolis parameter at different latitudes). F_l, F_c, and F_β correspond to the first, second and third terms in (2.8). All three forces decrease gradually in time.

The second is an integrated Coriolis force resulting from the (forever slowing) migration of the eddy toward the wall. The third is a southward β force resulting from the fact that as a particle circulates in a clockwise manner within the eddy, it senses a larger Coriolis force on the north side than it senses on the south side.

The above balance of forces holds regardless of the fluid's potential vorticity but requires the orbital velocities to be of $O(g'H_i)$; i.e., it requires the vortex to be intense. When the orbital velocities are weak, the time that it takes a particle to complete a single revolution is as long as the β adjustment time and, consequently, the time derivatives in (2.3) and (2.4) are no longer negligible.

3. Solution

To obtain the solution to the problem we introduce the expansions,

$$\psi = \overline{\psi} + \psi' + \cdots; h = \overline{h} + h' + \cdots \tag{3.1}$$

where the bars ($\overline{\ }$) denote association with a radially symmetric f-plane eddy and the primes denote distortions introduced by the presence of β (which forces the eddy to drift westward and encounter the wall). We shall see in the end of this section that the ratio of the perturbation (ψ', h', v') and the basic state ($\overline{\psi}$, $\overline{h}$, $\overline{v}$) is, at the most, of $O(\varepsilon^{1/2})$. Note that the "small distortion approximation" reflected in our expansion states (indirectly) that the so-called image effect is small. It implies that, at all times, only a small part of the circular eddy is distorted. As we shall see, our numerical simulations clearly support this

approximation. However, not all eddy-wall encounters display this behavior. For instance, quasi-geostrophic eddies (e.g., Shi and Nof, 1993) display an $O(1)$ shape distortion. The difference between the two distortions is related to the eddy inertia. In the intense eddy case discussed here, the inertia associated with the eddy's orbital motion is so large compared to the inertia associated with the westward drift that the wall effect is small. Namely, the role of the wall is merely to slow down the westward drift of the eddy and this has a relatively small effect on the eddy itself. By contrast, in the weak quasi-geostrophic cases, the two speeds (and inertias) are of the same order so that the effect of the wall is of $O(1)$.

a. Conservation of mass. Substitution of (3.1) into (2.1) and keeping only the first-order terms we find,

$$-\frac{d}{dt}\iint \overline{h}\,dxdy = \frac{g'}{2f_0}h_c^2 \qquad \text{which gives} \qquad \frac{16\pi f^2 R_d^3}{g'}\frac{dR_d}{dt} = \frac{-g'h_c^2}{2f_0}. \tag{3.2}$$

In deriving (3.2) it has been taken into account that the volume of a zero-potential vorticity eddy is $4\pi f^2 R_d^4/g'$ [because $h = H(t) - f^2r^2/8g'$ (see, e.g., Nof, 1981)]. As before, R_d is the time-dependent Rossby radius, $[g'H(t)]^{1/2}/f$.

b. Momentum flux. Substituting (3.1) into (2.8), neglecting products of the perturbations (and keeping in mind that, although within the leak the speed is high, the width of the leak is small), we get,

$$-\int_0^L h'(\overline{v})^2\,dx + C_x\iint_{\overline{S}} f_0\,\overline{h}\,dxdy + \beta\iint_{\overline{S}} \overline{\Psi}\,dxdy = 0, \tag{3.3}$$

where $\overline{S}$ is the area that the axisymmetric eddy would occupy on an f-plane. Recall that the width of the leak $L \sim O(\varepsilon^{1/2}R_{di})$ and that the thickness perturbations $h' \sim O(\varepsilon^{1/2}H_i)$ so that, as the continuity equation implies, the first-term (i.e., the rocket force) is of the same order as the other terms. Note also that along the eddy edge the velocity is $-fR/2$ [where R is the eddy radius] because $h = 0$ along the edge so that the Bernoulli implies that $u^2 + v^2 =$ constant. Taking again into account the known velocity and depth profiles of a radially symmetric zero potential vorticity eddy, we find that (3.3) takes the form,

$$-\frac{\sqrt{2}}{16\pi}(g')^2h_c^2 + \sqrt{2}\,R_d^3f_0^3\frac{dR_d}{dt} + \frac{\beta}{3}R_d^5f_0^3 = 0. \tag{3.4}$$

Note that the condition $C_x \approx dR/dt$ has also been used and that L, the width of the (narrow) leak, has been computed from geostrophy taking $\overline{v}$ to be a constant. Note also that the relationship $C_x \approx dR/dt$ involves the plausible assumption that the eddy progresses toward the wall at the same rate that its radius is reduced; i.e., it peels and sheds fluid like an onion and is forever in touch with the wall.

Elimination of h_c^2 between (3.2) and (3.4) gives a single differential equation for R_d,

$$-\frac{dR_d}{dt}=\frac{\beta R_d^2}{9\sqrt{2}}.$$

The solution obeying the initial condition $R_d = R_{di}$ at $t = 0$ is,

$$\boxed{R_{\mathrm{d}}=\frac{R_{di}}{1+\beta R_{di}t/9\sqrt{2}}} \tag{3.5}$$

Relation (3.5) implies that the decay of the central depth H is

$$\boxed{H = H_i/\,[1+\sqrt{2}\,\beta R_{di}t/18]^2} \tag{3.6}$$

and that the decay of the eddy's radius is,

$$\boxed{R = R_i/\,[1+\beta R_i t/36].} \tag{3.7}$$

Finally, we find that the eddy loses its mass at a rate of

$$\frac{\pi\beta f'^2 R_i^5}{144g'}\Big/\left(1+\frac{\beta R_i t}{36}\right)^5,$$

and that the eddy migrates toward the wall at a rate of $-2\beta R_d^2/9$, which is a third of its open ocean propagation rate $[-2\beta R_d^2/3]$. Substitution of our solution into the equations that we started with (2.2–2.3) verifies that, as required, all of the neglected terms are indeed small. This completes the general derivation of the analytical solution for the encounter of a zero potential vorticity eddy.

Before proceeding to the numerics, there is one more aspect that we need to deal with. This is the question of how large is the migration along the wall. By applying the procedure that we already performed for the meridional balance of forces to the zonal balance of forces we find

$$-f\iint C_y h\,dxdy=\frac{g'}{2}\int_B^D h^2dy, \tag{3.8}$$

where the term on the left-hand side represents the zonal-integrated Coriolis force resulting from the meridional migration of the entire eddy C_y and the term on the right-hand side is the zonal pressure force resulting from the nonzero thickness along the wall $[O(\varepsilon^{1/2}H_i)]$.

It is easy to see that, due to the problem geometry, the distance BD is of $O(\varepsilon^{1/4}R_{di})$ (see Fig. 1). Consequently, (3.8) gives $C_y \sim O[\varepsilon^{5/4}(g'H_i^{1/2}]$ which is smaller than C_x; i.e.,

$C_y \sim O(\varepsilon^{1/4} C_x)$. This means that, mathematically, it is correct to ignore C_y because it is of an order higher than the other speeds. Realistically, however, we expect to see some slow migration toward the equator because $\varepsilon^{1/4}$ is not that small. (For our numerical experiment described in Section 4 it is embarrassingly as high as 0.7! Having stated this, however, we should also state that using an ε which is almost as large as a unity is common. For instance, it is routinely employed in the application of quasi-geostrophic theory to eddies and rings.) Our numerical simulations will show that there is indeed a small migration away from the poles. The speed is nevertheless smaller than C_x and, during the entire encounter, the eddy progresses meridionally less than half a radius.

4. Numerical simulations

To further analyze the validity of our assumptions (e.g., that the flow is parallel to the wall downstream), we shall now present numerical simulations and quantitatively analyze the results.

a. Numerical model description. We used the Bleck and Boudra (1986) reduced gravity isopycnic model with a passive lower layer and employed the Orlanski (1976) second-order radiation conditions for the open boundary in the south. We found that this condition is satisfactory because the downstream streamlines were not disturbed when they crossed the boundary. To speed up the experiments (which make our runs more economical) and reduce the effect of friction, we used a magnified value for β in most of our experiments. Specifically, we performed two kinds of experiments. The first kind were high resolution experiments with an intense zero potential vorticity eddy subject to a magnified β. The second group was made up of relatively low resolution experiments with a weak varying potential vorticity eddy subject to a regular β.

Within each group the results were very similar to each other and, consequently, we present here only one experiment of each group. Since each run provides numerous data points we believe that this presentation is adequate. As is typical for these kinds of experiments, our wall was slippery[3] and we took the vorticity to be zero next to it. We began the experiment by setting an *f*-plane eddy next to the wall at $t = 0$. The first few days involved not only the *f*-plane eddy adjustment to the presence of the β but also an initial adjustment to the presence of the wall.

The zero potential vorticity run that we present was conducted with a (magnified) β of 2.3×10^{-10} m^{-1} s^{-1} and a relatively high resolution corresponding to $\Delta x = \Delta y = 3$ km. The initial eddy radius was 84 km, and, for numerical stability, we chose an eddy viscosity of 200 m^2 s^{-1}; the time step was 135 sec and the initial eddy central thickness was 510 m. These choices are certainly adequate for a Rossby radius of 30 km (corresponding to a g' of 9.8×10^{-3} ms^{-2} and $f_0 = 7.3 \times 10^{-5}$ s^{-1}) and a Munk layer thickness $[(\upsilon/\beta)^{1/3}]$ of about

3. Experiments with no-slip walls were also conducted; they are virtually indistinguishable from the free-slip experiments.

10 km. Furthermore, these choices always allowed for at least three grid points across the leakage, which is also adequate.

To simulate some of the effects of a sloping bottom we also performed a series of experiments in which we introduced a uniform southward advection. Such advection is, of course, not a true representation of topographic effects (which require at least two active layers and are an entirely different problem). Nevertheless, it does give some indication of what the results might be. We found that, as expected, very strong advection changes the results altogether but even an advection as large as the eddy migration rate has practically no influence on the results. This particular advection influence is shown (in the appropriate figures) together with the other results.

The varying potential vorticity run was conducted with a regular β (2×10^{-11} m^{-1} s^{-1}), a much larger eddy radius of 280 km, a somewhat lower resolution (a grid size of 15 km), a time step of 864 sec and an eddy viscosity of 400 m^2 s^{-1}. Again, these choices are adequate for a Rossby radius of 49 km (based on an initial central thickness of 1700 m). However, because we used a regular value for β, the Munk layer thickness was considerably larger (27 km compared to 10 km in the previous experiment) and the complete encounter with the wall lasted much longer than in the intense zero potential vorticity case (440 days compared to 40 days). Here, the initial Rossby number was 0.07 (compared to 0.5 in the zero potential vorticity case). The initial velocity profile was approximately linear up to ¾ of the ring radius; from this point it fell rapidly (also in an approximately linear manner) to zero along the edge.

Since the Rossby number is now of the same order as the parameter $\beta R_d/f_0$, there is no longer a fast and slow time. Instead, the time that it takes a particle to complete a single revolution is of the same order as the decay time scale $(\beta R_d)^{-1}$. Consequently, we do not expect that the time derivatives in the momentum equations can be neglected implying that the balance given by (2.8) is not relevant for this case.

b. Results. The results of the first set of experiments (intense zero potential vorticity eddy) are shown in Figures 3–10. All show an excellent agreement with the theory. This is remarkable considering the fact that the error in the perturbation expansion is of $O(\varepsilon^{1/2})$ which, for our numerical choices, is roughly 0.5. The reason for the relatively small deviations of the numerics from the analytics (despite the relatively large ε) is that the calculation is based on surface integrations which usually are not very sensitive to the eddy's shape because they smooth out the errors. We note that (as expected), upon encountering the wall, the eddy's westward drift speed is gradually reduced and that, after an initial period of adjustment (which, as expected, lasts for a few days) the agreement between the theory and experiment is excellent (Fig. 4).

The same can be said of the eddy volume (Fig. 5), the central depth (Fig. 6), the radius (Fig. 7), and the mass-flux via the leak (Fig. 8). The most pronounced effect of friction is to reduce the orbital speeds along the eddy rim and the associated speeds within the leak. This is particularly noticeable during the first part of the encounter when the eddy still has a

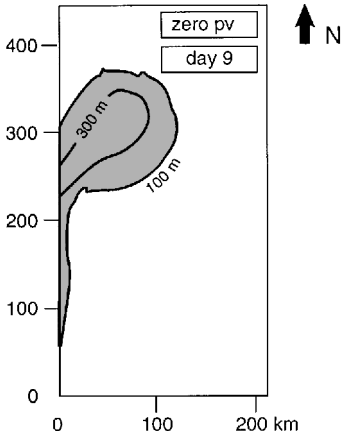

Figure 3. Depth contours (meters) of a zero potential vorticity eddy [subject to a magnified β (12×10^{-11} m^{-1} s^{-1})] nine days after encountering a wall. Note the leak along the wall. Physical constants: $f_0 = 7.3 \times 10^{-5}$ s^{-1}; $g' = 9.8 \times 10^{-3}$ m s^{-2}; $H_i = 510$ m; $\varepsilon = 0.051$. Grid size $\Delta x = \Delta y = 3$ km; time step $\Delta t = 135$ sec. The eddy viscosity was $\upsilon = 200$ m^2 s^{-1}.

relatively large volume so that its rim velocity is still relatively high. (Recall that, for a zero potential vorticity eddy, the maximum orbital speed is along the rim.) As a result of this frictional reduction, both the leak's mass flux and the force associated with the leak are a bit smaller than the theoretically predicted values (Figs. 8, 9, and 10). As expected, this difference between the theoretical and the actual mass fluxes decreases as the encounter continues because the eddy's size and its associated rim velocities decrease (Fig. 8). It should be clear by now that the frictional effect (which causes a reduced leakage) explains why the theoretical volume, radius, and central depth all decay more rapidly than the actual numerical values (Figs. 5, 6, and 7).

The results of the second set of experiments (weak, varying potential vorticity eddy) are shown in Figures 11–12. As in the zero potential vorticity case, the eddy displays a leak along the wall. However, in contrast to the zero potential vorticity case, in this experiment the time that it takes a particle to complete a single revolution [$\sim O(R_0 f)^{-1}$ (where R_0, the Rossby number, is roughly 0.07)] is of the same order as the encounter time [$\sim O(\beta R_d)^{-1}$]. As a result, the slowly varying approximation is no longer relevant. Also, since β is smaller (resulting in a larger ratio between the Munk layer thickness and the eddy radius) and the encounter time is much longer than in the zero potential vorticity case, friction is much more important. Because of both of these aspects, the deviations of the numerically simulated forces from the theoretically predicted balance are much greater (Fig. 12) than those in the zero potential vorticity case (Fig. 10).

Recently, the author has learned of the numerical experiments of Zavala Sansón, Graef and Pavia which were published at the end of 1998 after the original submission of this article. They dealt with constant vorticity (nonuniform potential vorticity) lenses and use the so-called particles in cell method to compute the interaction process. Their results are consistent with the present calculations. Their eddy stays almost circular and leaks

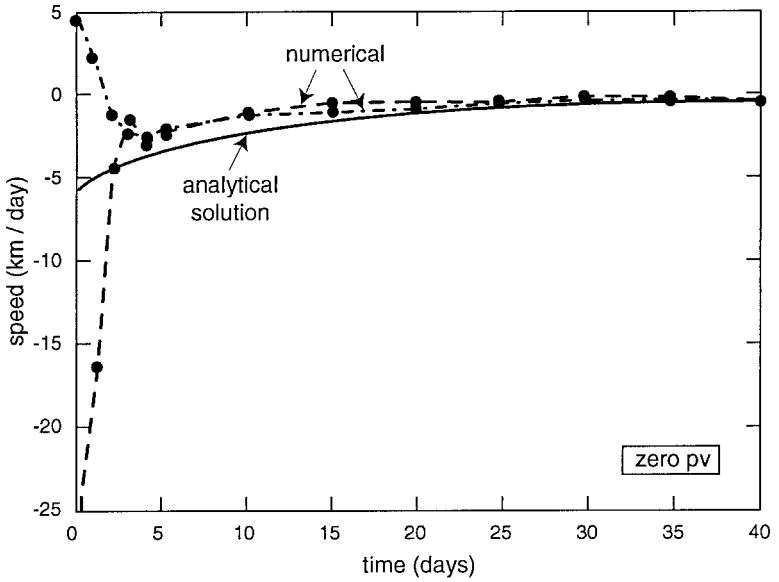

Figure 4. The analytically predicted migration speed (solid line), the numerically calculated speed based on the gradually decreasing mean eddy radius (dashed-dotted line), and the numerically calculated speed based on the migration of the maximum thickness (dashed line). The eddy is the same eddy shown in Figure 3; it has zero potential vorticity. Note that during the first few days the eddy goes through an adjustment process (not described by our model). Consequently, during this stage the agreement between the theory and the experiment is not so good. After the adjustment is completed (say, at day 3), however, the agreement between the analytical prediction and the numerical simulation is excellent. Note that the (absolute) numerical values are slightly lower than the analytical ones because friction slows down the orbital speed and, consequently, the westward drift is also reduced.

equatorward during the entire interaction process. [Note, however, since Zavala Sansón *et al.* (1998) deal with eddies whose potential vorticity is not zero, a detailed comparison of their results to ours is impossible.] Although their article does not contain an analytical solution, they did derive a relationship analogous to (3.8) [see (their) equation (18)].

c. Limitations. As is frequently the case, both the analytical and the numerical model have their limitations. The three most important weaknesses of the analytical solution result from the slowly varying assumption, the fact that we did not find the complete first-order solution, and the use of a layer-and-a-half model. (Note that the latter limitation is also present in the numerics.) We shall take these three issues one by one.

The first assumption eliminates the contribution of the time-dependent terms to the long-shore momentum-flux. The assumption has been used successfully before and is valid as long as the encounter time is much longer than the orbital time. However, although the assumption is reasonable, it essentially excludes weak and slow eddies from the model because the orbital time of these eddies is of the same order as the encounter time. The

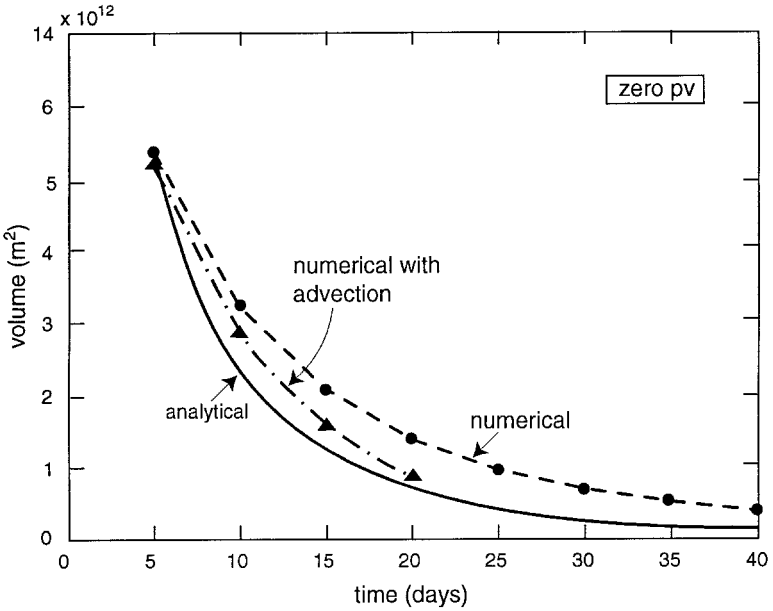

Figure 5. As in Figure 4 except that here we show a comparison between the analytically predicted volume as a function of time (solid line) and the corresponding numerical values (dashed line). As before, the agreement is excellent. Note that the numerically simulated volume reduction (in time) is slightly smaller than the analytically predicted reduction. Again, this is due to friction which is most effective along the rim where the speeds are high. This is to say, as a result of friction, both the high speeds along the eddy rim and the leak's speeds (which are of the same order as the speed along the rim) are reduced. Consequently, less fluid is draining from the vortex and the eddy loses its volume more slowly. We shall see later (Fig. 8) that, by the time that we reach day 15 or so, the eddy has lost much of its original size so that the velocities along the rim are no longer high and, as a result, the role of friction is minimal. For a comparison we also show the numerical results for an eddy advected along the coast at a speed equal to its initial propagation rate toward the wall (dashed-dotted line). This experiment was cut off at day 20 because by that time the eddy was swept out of the domain.

second limitation can be important because the complete first-order solution may impose constraints which may restrict the validity of our solution. Our third limitation (resulting from the one-and-a-half layer approach) excludes baroclinic instabilities (of both the eddy and the downstream current) and prevents the eddy from radiating energy outward (e.g., Flierl, 1984). This essentially eliminates a nonfrictional decay from the problem.

5. Discussion and summary

The foregoing theory is applicable to various situations because almost all westward drifting eddies ultimately collide with western walls. For example, warm-core Gulf Stream rings collide with the North American Continent, Meddies collide with the Great Meteor Seamounts, and Agulhas rings probably collide with the South American Continent. [Such an encounter has not been directly observed but seems to be inevitable; it is, nevertheless,

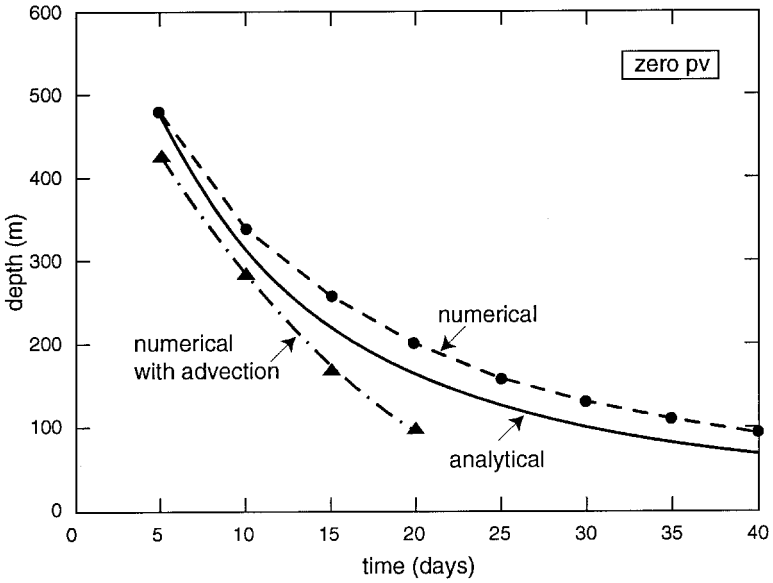

Figure 6. As in Figure 4 except that here we compare the analytical prediction for the central thickness (solid line) and the corresponding numerical values (dashed line). As before, the agreement is excellent. As in Figure 5 we also show the numerical results for an eddy advected along the shore (dashed-dotted line).

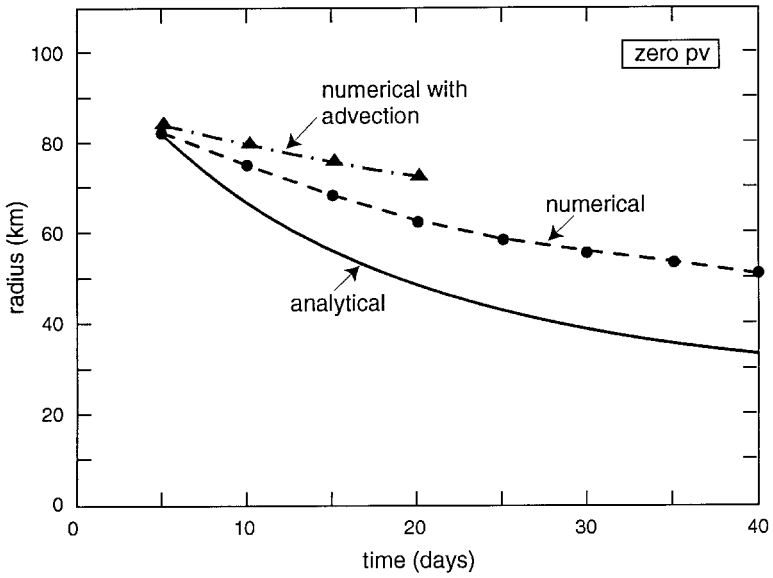

Figure 7. As in Figure 4 except that we compare the analytical and numerical radii. Again, the numerical eddy decays more slowly than the analytical one. This is due to friction which reduces the mass flux via the leak during the initial stages of the encounter when the velocities along the rim are still high (see Fig. 8). As in Figure 5 we also show the numerical values for an eddy advected along the coast.

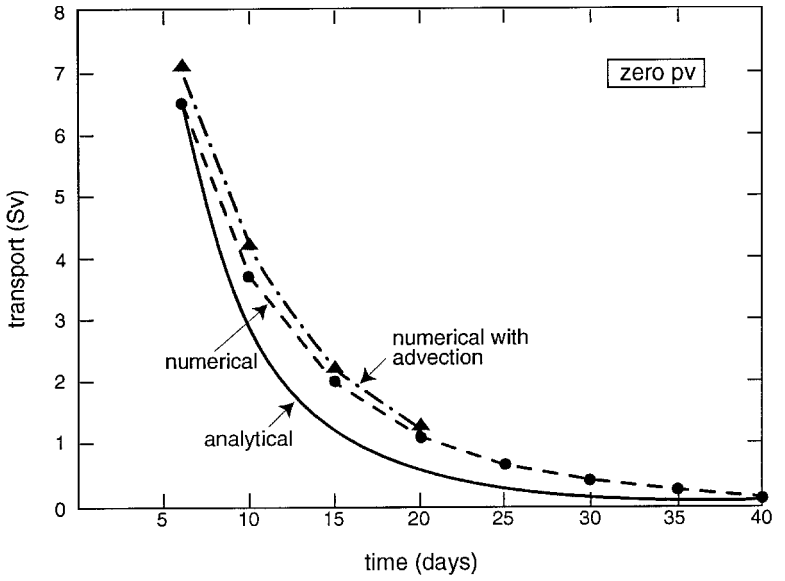

Figure 8. As in Figure 4 except that here we compare the analytical and numerical mass flux via the leak. In the beginning of the experiment the eddy is still large and, consequently, the velocities along the rim are still high. As a result, friction has a relatively large effect and the velocities along the rim are significantly reduced. This, combined with the fact that the leak is very narrow, produces the large initial (i.e., day 5 to, say, day 16) difference between the analytical prediction and the smaller numerical values. Later on (after, say, day 16) friction becomes less important and other effects enter the process. The transport was measured along the northern boundary shown in Figure 3. The analytical and the numerical transports were aligned at the time that the numerical transport abruptly rises from zero to its maximum value. As in Figure 5, we also show the numerical values for an eddy advected along the shore (dashed-dotted line).

complicated by the presence of the Brazil Current (e.g., Byrne *et al.,* 1995).] In all of these three cases, most of the continental rise variation scale $\sim O(10\,\text{km})$ is typically much smaller than the size of the rings ($\sim$100 km) suggesting that the vertical wall approximation is plausible [see Fig. 13 and Csanady (1979) (his) Fig. 3, Richardson and Tychensky (1998) (their) Fig. 9] considered to be the "wall." For the Gulf Stream and the Agulhas case the top of the continental rise (wall) is below the surface, so that the leakage that we speak about is subsurface as well and, consequently, cannot be detected from space. Furthermore, its relatively small size makes its identification from *in situ* measurements fairly difficult. It is hoped, however, that this study will encourage observational attempts to identify such leaks.

The results of our theory can be summarized as follows:

1. The inviscid encounter of an intense lens-like eddy with a meridional wall involves two time scales, a fast time scale [i.e., the orbital time scale $O(f^{-1})$] and a slow time scale [i.e., the time that the vortex is forced against the wall which equals the diameter of the vortex divided by its time-dependent westward drift; $O(\beta R_d)^{-1}$]. As a

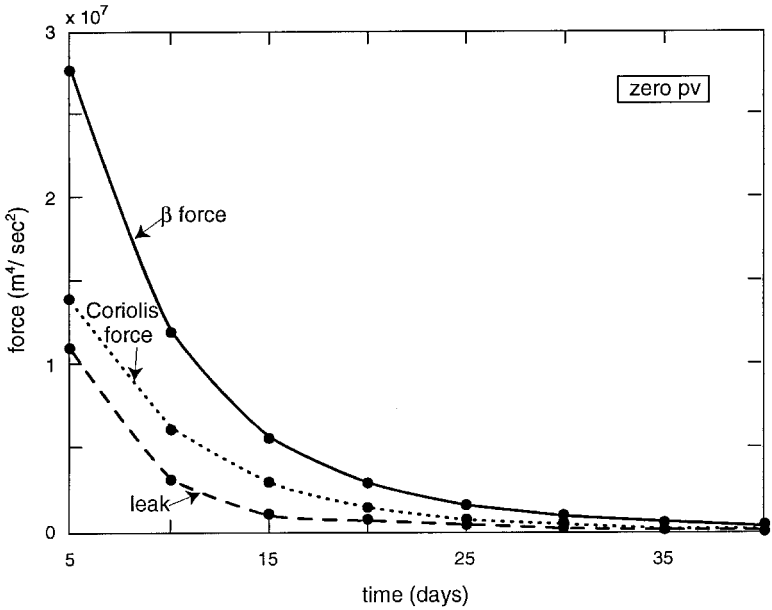

Figure 9. The meridional forces acting on the eddy shown in Figures 4–8 as a function of time. The integrated β-induced force ($\beta\int\int y\,dxdy$) is shown with the solid line, the integrated Coriolis force ($fCx\int\int h\,dxdy$) with the dotted line, and the integrated leak-rocket effect ($\int hv^2dx$) is shown with the dashed line. According to our analytical solution, the sum of the two latter forces should equal the former force. As more clearly demonstrated in Figure 10, this balance clearly holds.

result of these two time scales, the eddy-wall problem can be treated analytically as a slowly varying process (implying that all the derivatives with respect to time can be ignored in the momentum equations). For simplicity, we focus on zero potential vorticity eddies. Such eddies have a linear velocity profile (with a shear of $-f/2$) so that their maximum speed is along their periphery.

2. The analytical solution (3.5–3.7) corresponds to a balance between three meridional forces, the equatorward β-induced force, the poleward "rocket" force resulting from the leak, and the poleward integrated Coriolis force resulting from the (forever decreasing) westward movement of the eddy (Fig. 2).

3. The nonlinear analytical solution shows that the eddy's westward speed, volume, radius, and central depth all gradually decrease as $1/(\beta R_d)^{-1}t$ (see Figs. 4–7) implying that it takes quite a bit of time for the eddy to completely leak out and lose its identity as a coherent feature. A typical intense eddy would lose 70% of its volume within 200 days or so.

4. In addition to the forever slowing westward migration of the eddy into the wall [$O(\beta R_d^2)$], there is a very weak equatorward migration along the wall. This migration

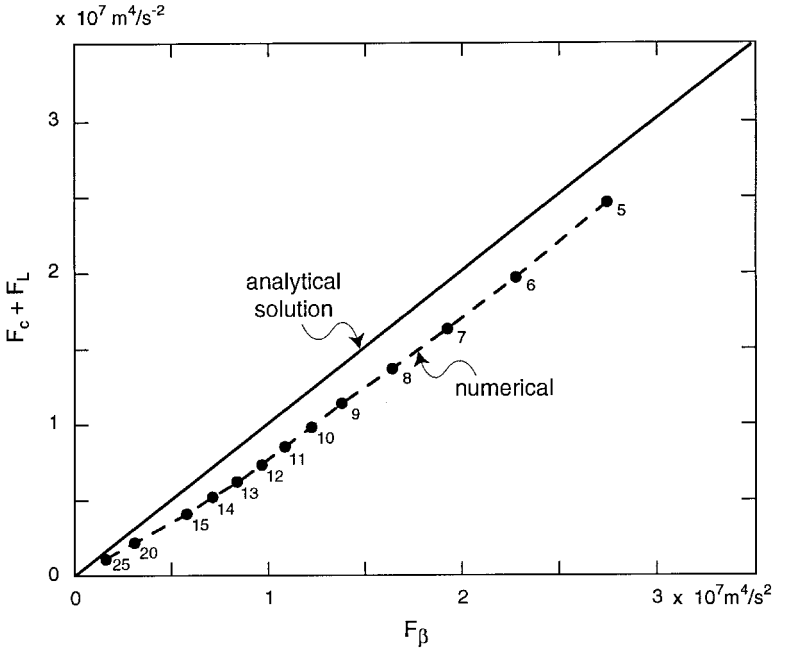

Figure 10. As in Figure 9 except that here we plotted the sum of the integrated Coriolis force and the rocket force on the vertical axis and the β force on the horizontal axis. (Numerals next to the dots indicate the day.) According to our analytical solution, all the numerically simulated values should fall on the solid line corresponding to the balance of the three forces. We see that this is indeed the case. As expected, the sum of the Coriolis force and the force due to the leak are slightly smaller than the β force (because of the friction-induced reduction in the leaked mass flux).

$[\sim O(\beta R_d/f\ )^{5/4} f R_d]$ is smaller than our largest calculated speed $[\sim O(\beta R_d^2)]$ and, consequently, is not a part of our solution.

5. Numerical simulations using the Bleck and Boudra model are in excellent agreement with the analytical solution (see again Figs. 4–7 as well as Fig. 8). They also illustrate that the balance of the three forces associated with the analytical solution is indeed valid (Figs. 9–10).

6. Since frictional forces are most pronounced in regions of high velocities (i.e., the rim), they tend to reduce the leakage mass flux. Consequently, frictional forces tend to slow down the draining process in the beginning of the encounter when the eddy is still large and the rim velocities are still high (Fig. 8). Later on the effects of friction are much less pronounced.

7. Weak eddies (i.e., eddies whose orbital speed is small so that there is no longer a fast time scale) display similar general characteristics to intense eddies (Figs. 11–12).

As already mentioned, it is hoped that observational attempts will be made to either support

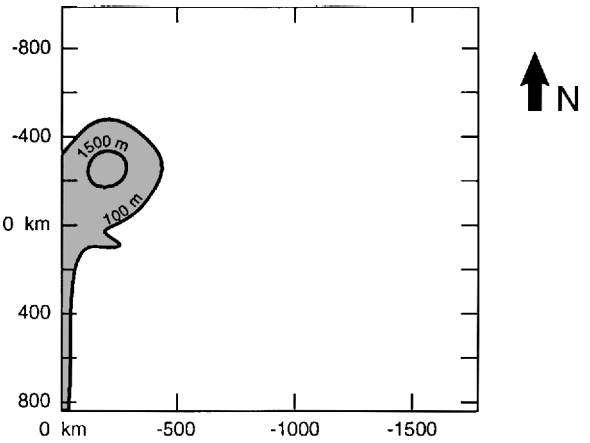

Figure 11. Depth contours (in meters) for an encounter of an eddy with a finite (nonzero) potential vorticity. As before, the eddy leaks as it encounters the wall. However, in contrast to the zero potential vorticity case, the earlier balance of the three quasi-steady forces is not valid for this case (Fig. 12). This is due to the breakdown of the slowly varying approximation. Physical constants: $\beta = 2 \times 10^{-11}$ m s^{-1}; $f_0 = 8.4 \times 10^{-5}$ s^{-1}; $g' = 9.8 \times 10^{-3}$ m s^{-2}; $H_i = 170$ m. The grid size was $\Delta y = 15$ km and the time step was 864 sec; the eddy viscosity was $\upsilon = 400$ m^2 s^{-1}.

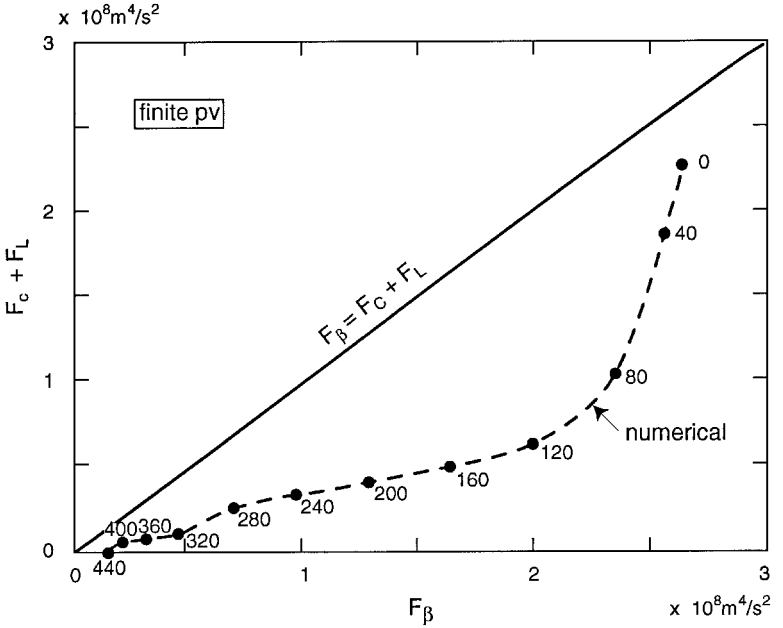

Figure 12. As in Figure 10 except that the forces for the relatively weak finite potential vorticity eddy are shown. Here the dots are quite far from the solid line (corresponding to a balance between the three quasi-steady forces) because the slowly varying approximation is no longer valid and, consequently, the time dependent derivatives are no longer negligible.

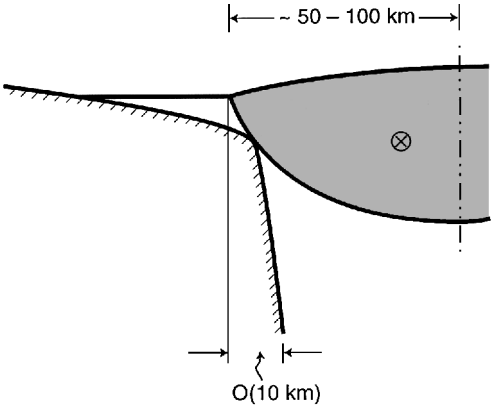

Figure 13. A schematic cross-section of a (homogeneous) lens adjacent to a steep continental rise. Here, the slope of the continental rise is much greater than the slope of the lens interface. Consequently, replacing the boundary by a vertical wall is appropriate as a first approximation. Note, however, that since the actual rings are stratified, the wall-induced leak will be primarily noticed below the surface (along the continental break).

or reject our newly developed theory. It is also hoped that the study will encourage more concrete numerical investigations.

Acknowledgments. This study was supported by the National Science Foundation under contracts OCE 9503816 and 9633655, National Aeronautics and Space Administration grants NAGW-4883, NAG5-4813 and NAG5-7630, and Office of Naval Research grant N00014-89-J-1606.Computations were made by S. Van Gorder.

APPENDIX

List of symbols

C_x, C_y time-dependent migration rate in the x and y directions
f Coriolis parameter ($f_0 + \beta y$)
g' "reduced gravity," $(\Delta\rho/\rho)g$
h upper layer thickness
h_c thickness of light water within the leak at point c, $O(\varepsilon^{1/2}H)$
H central eddy thickness
L width of the leak, $O(\varepsilon^{1/2}R_d)$
q draining mass flux
R eddy radius, $O(R_d)$
R_d Rossby radius $[(g'H)^{1/2}/f]$
s vortex area
S integration area, $O(R_d^2)$
t time, "fast" time is $O(f^{1})$, "slow" time is $O(\beta R_d)^{-1}$
u, v velocities in Cartesian coordinates, $O(fR_d)$ within the eddy
$\overline{u}$, $\overline{v}$ speeds in the absence of the wall

u', v' perturbations due to the encounter with the wall
V eddy volume
β variation of the Coriolis parameter with latitude
ε small parameter equal to $\beta R_d/f_0$; it is much smaller than unity
ϕ boundary of integration area S
ψ streamfunction (defined by $\partial\psi/\partial y = -uh$; $\partial\psi/\partial x = vh$)
υ eddy viscosity
$\oint$ counterclockwise integration
i subscript denoting the "initial" state prior to the encounter

REFERENCES

Bleck, R. and D. Boudra. 1986. Wind-driven spin-up in eddy-resolving ocean models formulated in isopycnic and isobaric coordinates. J. Geophys. Res., *91,* 7611–7621.

Byrne, D. A., A. L. Gordon and W. F. Haxby. 1995. Agulhas eddies: A synoptic view using Geosat ERM data. J. Phys. Oceanogr., *25,* 902–917.

Csanady, G. T. 1979. The birth and death of a warm-core ring. J. Geophys. Res., *84,* 777–780.

Flierl, G. 1979. A simple model of the structure of warm and cold-core rings. J. Geophys. Res., *84,* 78–85.

—— 1984. Rossby wave radiation from a strongly nonlinear warm eddy. J. Phys. Oceanogr., *14,* 47–58.

Killworth, P. D. 1983. On the motion of isolated lenses on a beta-plane. J. Phys. Oceanogr., *13,* 368–376.

Masuda, A. 1988. A skewed eddy of batchelor-modon type. J. Ocean. Soc. Japan, *44,* 189–199.

Masuda, A., K. Maribayashi and M. Ishibashi. 1987. Bachelor-modon type eddies and isolated eddies near the coast on an *f*-plane. J. Ocean. Soc. Japan, *43,* 383–394.

Minato, S. 1982. Geostrophic adjustment near the coast. J. Ocean. Soc. Japan, *38,* 225–235.

—— 1983. Geostrophic response near the coast. J. Ocean. Soc. Japan, *39,* 141–149.

Nof, D. 1981. On the β-induced movement of isolated baroclinic eddies. J. Phys. Oceanogr., *11,* 1662–1672.

—— 1988a. Draining vortices. Geophys. Astrophys. Fluid Dyn., *42,* 187–208.

—— 1988b. Eddy-wall interactions. J. Mar. Res., *46,* 527–555.

Olson, D. B. 1991. Rings in the ocean. Ann. Rev. Earth Planet. Sci., *19,* 283–311.

Orlanski, I. 1976. A simple boundary condition for unbounded hyperbolic flows. J. Comp. Phys., *21,* 251–269.

Richardson, P. L. and A. Tychensky. 1998. Meddy trajectories in the Canary Basin measured during the SEMAPHORE experiment, 1993–1995. J. Geophys. Res., *103,* 25,029–25,045.

Shi, C. and D. Nof. 1993. The splitting of eddies along boundaries. J. Mar. Res., *51,* 771–795.

—— 1994. The destruction of lenses and generation of wodons. J. Phys. Oceanogr., *24,* 1120–1136.

Umatani, S. and T. Yamagata. 1987. Evolution of an isolated eddy near a coast and its relevance to the "Kyucho." J. Ocean. Soc. Japan, *43,* 197–203.

Yasuda, I., K. Okuda and Keisuke Mizuno. 1986. Numerical study on the vortices near boundaries: Considerations on warm core rings in the vicinity of east coast of Japan. Bull. Tohoku Reg. Fish. Res. Lab., *48,* 67–86.

Zavala Sansón, L., F. Graef and E. G. Pavia. 1998. Collision of anticyclonic, lens-like eddies with a meridional western boundary. J. Geophys. Res., *103,* 24,881–24,890.

Received: *8 September, 1998;* revised: *29 June, 1999.*